

RELIABILITY OF BASEMENTS AND STRUCTURES IN CRYOLITHOZONE

DOI: 10.21782/EC2541-9994-2018-5(51-56)

HORIZONTAL EVAPORATOR TUBE (HET) THERMOSYPHONS:
PHYSICAL-MATHEMATICAL MODELING AND EXPERIMENTAL DATA, COMPAREDA.A. Ishkov¹, G.V. Anikin¹, G.M. Dolgikh², S.N. Okunev²¹Earth Cryosphere Institute, SB RAS, P/O box 1230, Tyumen, 625000, Russia; a.ishkov1988@yandex.ru, anikin@ikz.ru²OOO NPO "Fundamentstroyarkos", 12, Novatorov str., Tyumen, 625014, Russia; fsa@npo-fsa.ru

New experiments have provided data necessary for designing thermosyphons with horizontal evaporator tubes (HET systems). A physical-mathematical model with different input parameters was used to describe the operation of a HET system in various modifications. The model includes temperature excess in the working fluid as a correction added to the previous model version to improve the fit between the computed and measured average evaporator temperatures. The excess temperatures have been estimated for different configurations of HET systems charged with ammonia.

Thermal stabilization, soil, temperature field, overheating, thermosyphon, HET system

INTRODUCTION

As oil and gas resources in West Siberia become progressively more exhausted and hard to recover, the East Siberian Subarctic and Arctic reservoirs arouse ever greater interest of investors. Active development of these reservoirs requires extensive construction of production and utility structures. However, construction in high latitudes may face problems associated with degradation of permafrost and related loss of its bearing capacity. The unwanted effects can be mitigated using various systems that keep the ground frozen for the lifetime of the structures, which operate as a "heat diode": conduct cold in winter and stop working in summer. Currently, many various refrigeration systems have been in use, such as single and deep thermosyphons; systems based on natural convection (two-phase thermosyphons) with vertical and horizontal evaporator tubes (VET and HET, respectively); drain systems, etc. [Dolgikh *et al.*, 2008].

Before coming into the construction practice, such systems were used for cooling equipment units in chemical, nuclear power, and steel making industries [Kutepov *et al.*, 1986; Pioro *et al.*, 1991], where thermal loads are orders of magnitude greater than in the heat transfer processes in foundation soils.

This study focuses on the operation of an HET experimental system with different input parameters of tube length, condenser height, specific thermal load, and condenser temperature [Dolgikh and Okunev, 1989]. The experiments yield average evaporator temperatures which are compared with the results of physical-mathematical modeling. The comparison of measured and computed evaporator tem-

peratures in HET systems of different configurations allows estimating the excess temperature of the working fluid.

HET THERMOSYPHON SYSTEMS

The experimental installation used for estimation of the HET system parameters with tube lengths from 200 to 800 m is a field-size thermosyphon with one plastic tube of a variable length [Dolgikh and Okunev, 1989]. The system operates as a two-phase thermosyphon with unidirectional flow of the working fluid (coolant), ammonia in this case, composed of vapor and liquid phases (Fig. 1).

The system consists of an evaporator and a condenser. The evaporator is a plastic tube with heaters

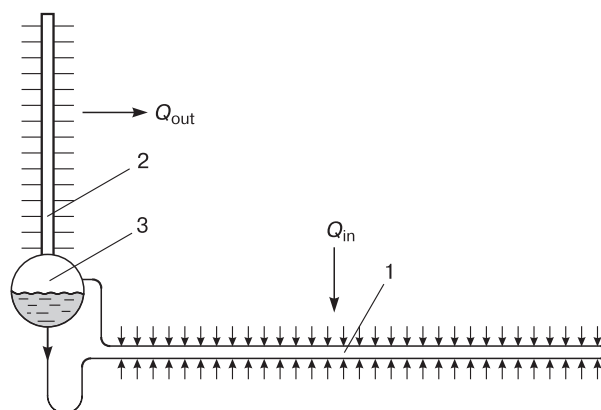


Fig. 1. An experimental HET system, general layout:

1 – evaporator; 2 – condenser; 3 – drain vessel; Q_{in} – input heat flux; Q_{out} – output heat flux.

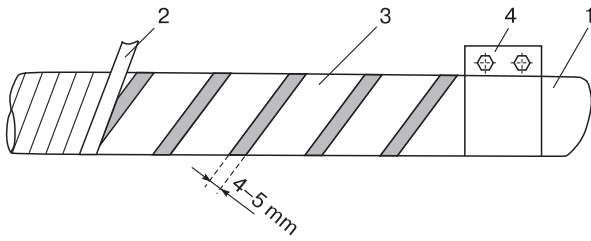


Fig. 2. Placement of heaters on evaporator tube:
 1 – polyethylene tube; 2 – insulating film; 3 – heater; 4 – clips.

mounted on its outer surface while the condenser is a welded assembly placed on a rack above the ground with an easily changeable height from 0.86 to 3.0 m. Cooling is performed by refrigerating compressors (2FU-I2) for the most precise setting of the condenser temperature.

The heaters are made as spiral aluminium foil, 63 mm wide and 0.065 mm thick, with a clearance of

4–5 mm between the turns (Fig. 2). They are protected from electricity and water effects with an insulating polyethylene film and are connected to a power source with clips. The evaporator tubes have a foam polyurithane coating, with Pt thermistors placed at every 25 m inside it. The resistance is measured by a digital bridge gauge (accurate to 0.01/0.05) according to the state standard requirements (GOST 19876-81). The temperature measurements are accurate to 0.1 °C.

METHODS

The experimental system was prepared for work in several steps:

- checking the density of working fluid (ammonia) at a pressure of 1.5 MPa;
- vacuuming to residual pressure no higher than 3 kPa;
- charging the system with fluid;
- checking the system for presence of air.

a

| Date | Fluid | Tube length | Drain vessel, m | Liquid level in condenser, mm | Air temperature, °C | Fluid temperature in condenser, °C | Average temperature of evaporator wall, °C | Specific heat flux, W/m |
|----------|---------|-------------|-----------------|-------------------------------|---------------------|------------------------------------|--------------------------------------------|-------------------------|
| 04.10.90 | Ammonia | 600 | 1.8 | 210 | 8.41 | -10.5 | -6.08 | 16.55 |

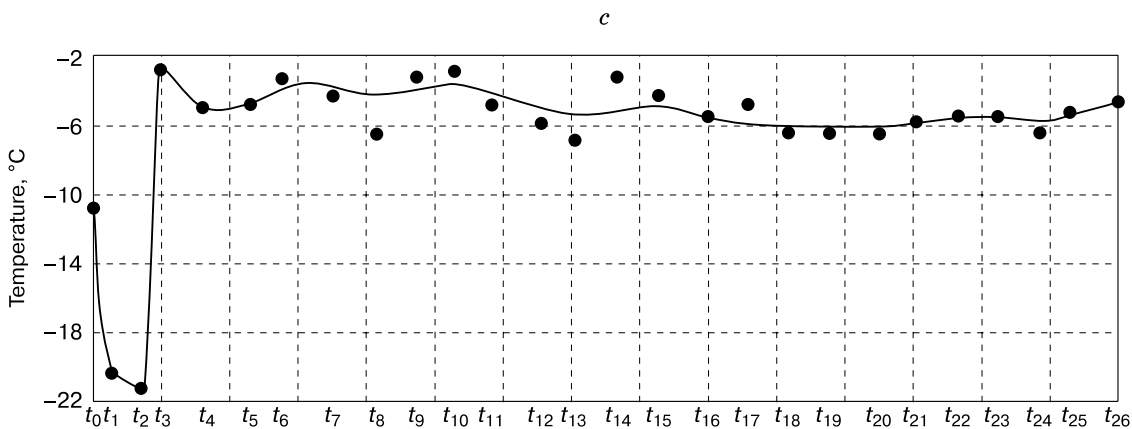
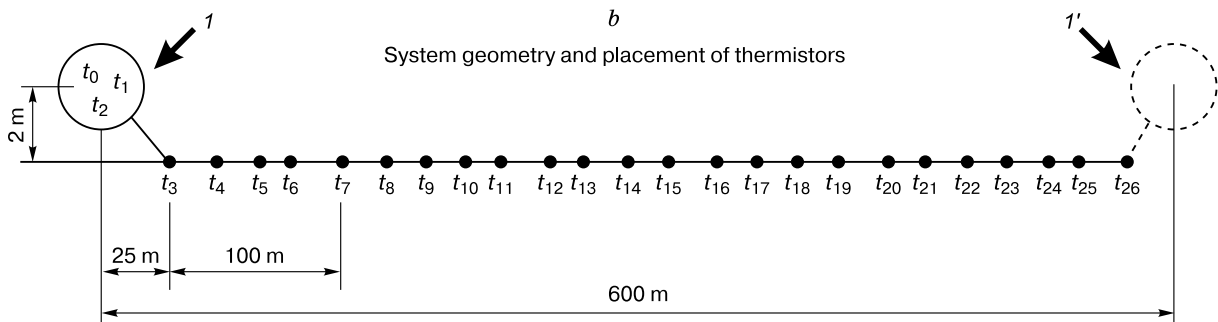


Fig. 3. Example data spreadsheet:

a – run data and input parameters; *b* – condenser height (1, 1') and placement of thermistors (t_1-t_{26}); *c* – temperatures along tube path. 1 – output evaporator segment; 1' – input evaporator segment.

The following parameters were varied:

- (1) tube length, from 200 to 800 m;
- (2) specific heat flux, from 9.46 to 57.10 W/m;
- (3) condenser (liquid column) height over the evaporator tubes, from 0.86 to 3.0 m.

We varied thermal loads by changing power supply to the heater and the hydraulic pressure by changing the condenser height.

The temperatures of the tube wall, condenser, and ambient air were measured by thermistors, which were placed on the evaporator to avoid distortion by heating; the thermistor sites were insulated and were not exposed to heating. The results were presented as a spreadsheet (see an example in Fig. 3).

RESULTS AND DISCUSSION

The operation of an HET system was described by a physical-mathematical model and the results were compared with experimental measurements. The system was modeled with the following input parameters: evaporator tube length (L_{ev}), condenser height above the tube (H_{con}), condenser temperature (t_{con} , °C), and specific thermal load on the evaporator (q , W/m) (Table 1).

The output parameters were average temperature at the evaporator wall and flow parameters of the two-phase (gas + liquid) working fluid. The evaporator temperature is especially important for this study as it is used to compare the measured and computed values (Fig. 4), in order to assess the modeling quality. This parameter was chosen because it is little variable along the tube path [Feklistov *et al.*, 2008]. The average temperature in physical-mathematical modeling was found as a sum of temperature values at each tube length step divided by the number of steps. In the experiment, averaging was performed by dividing the sum of temperatures at all thermistors by their number (Table 2).

Table 1. Input parameters for physical-mathematical modeling of HET system operation

| No. | L_{ev} , m | H_{con} , m | q , W/m | t_{con} , °C |
|-----|--------------|---------------|-----------|----------------|
| 1 | 800 | 3.00 | 9.46 | -2.25 |
| 2 | 400 | 0.86 | 11.85 | -1.99 |
| 3 | 200 | 1.80 | 28.55 | -6.50 |
| 4 | 400 | 0.86 | 9.50 | -3.70 |
| 5 | 400 | 0.86 | 13.47 | 11.75 |
| 6 | 400 | 1.67 | 14.03 | 8.61 |
| 7 | 600 | 3.00 | 12.05 | -4.25 |
| 8 | 600 | 1.80 | 9.35 | -3.75 |
| 9 | 200 | 3.00 | 32.50 | -5.00 |
| 10 | 400 | 3.00 | 31.68 | -10.50 |
| 11 | 200 | 3.00 | 57.10 | -15.00 |
| 12 | 400 | 1.67 | 21.89 | 11.98 |
| 13 | 200 | 1.80 | 48.10 | -15.00 |

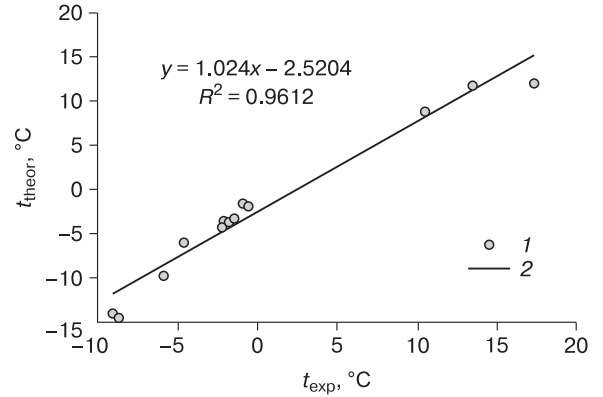


Fig. 4. Measured (t_{exp}) and computed (t_{theor}) average evaporator temperatures (1) and their least square approximation (2).

The data of the physical-mathematical model and the experiment are in a linear relationship (Fig. 4), with an approximation reliability (R^2) of 96.12 %. According to the trend equation, the calculated average evaporator temperature is 2.52 °C lower than the measured one, for two possible reasons: (i) heat loss in the tube thermal insulation and the effect of heaters on the thermistors, and (ii) earlier fluid boiling at some path segment by overheating. This happens in practice contrary to the assumption in the model that boiling starts only when the fluid reaches the boiling temperature at a saturation pressure. Since it is impossible to judge about the heat loss or the heating effect on measured temperatures (they commonly change smoothly within some range) in the experimental system which lacks the respective segments, the excess temperature of the fluid is assumed to be responsible for the misfit [Dolgikh and Okunev, 1989].

Table 2. Experimental and theoretical (modeling) results

| No. | L_{ev} , m | H_{con} , m | q , W/m | t_{con} , °C | t_{exp} , °C | t_{theor} , °C |
|-----|--------------|---------------|-----------|----------------|----------------|------------------|
| 1 | 800 | 3.00 | 9.46 | -2.25 | -0.87 | -1.55 |
| 2 | 400 | 0.86 | 11.85 | -1.99 | -0.53 | -1.78 |
| 3 | 200 | 1.80 | 28.55 | -6.50 | -4.67 | -5.99 |
| 4 | 400 | 0.86 | 9.50 | -3.70 | -2.06 | -3.47 |
| 5 | 400 | 0.86 | 13.47 | 11.75 | 13.42 | 11.89 |
| 6 | 400 | 1.67 | 14.03 | 8.61 | 10.50 | 8.91 |
| 7 | 600 | 3.00 | 12.05 | -4.25 | -1.82 | -3.49 |
| 8 | 600 | 1.80 | 9.35 | -3.75 | -1.54 | -3.29 |
| 9 | 200 | 3.00 | 32.50 | -5.00 | -2.18 | -4.17 |
| 10 | 400 | 3.00 | 31.68 | -10.50 | -5.95 | -9.67 |
| 11 | 200 | 3.00 | 57.10 | -15.00 | -9.05 | -13.95 |
| 12 | 400 | 1.67 | 21.89 | 11.98 | 17.37 | 12.24 |
| 13 | 200 | 1.80 | 48.10 | -15.00 | -8.65 | -14.36 |

The operation of an HET system is considered further using the parameter of a relative evaporator length for convenience:

$$y = \frac{x}{L_{ev}},$$

where L_{ev} is the evaporator tube length; x is the distance from the evaporator input to the current point, ranging from 0 to L_{ev} . Thus, the relative evaporator length varies from 0 to 1.

The length of the heated evaporator segment (y_{max}) is given by

$$y_{max} = \left(\frac{\rho_L g H_{con} - \Delta p_{con}}{dP_{sat}/dt_{con}} \right) \frac{C_{pL} G_L}{U}, \quad (2)$$

where y_{max} is the relative path length from the evaporator input to the point where the fluid begins to boil, u.f.; Δp_{con} is the pressure gradient required to overcome friction, Pa; ρ_L is the density of the liquid fluid phase, kg/m³; g is the gravity acceleration; H_{con} is the height of the condenser, m; C_{pL} is the specific heat capacity of the liquid at constant pressure, J/kg; G_L is the fluid flow rate within the heating segment, l/h; dP_{sat}/dt_{con} is the pressure of saturated vapor as a function of condenser temperature, Pa; U is the total heat output to the evaporator, W.

The main equation for the operation of an HET refrigeration system is [Anikin et al., 2011]:

$$\begin{aligned} & \varphi_G(1)(\rho_L - \rho_G)gH_{con} = \\ & = \frac{\xi(\text{Re}_L, \bar{\Delta})(L_y + L_{un} + y_{max}L_{ev})}{D} \frac{G_L^2}{2S_{tr}^2\rho_L} + \\ & + \int_{y_{max}}^1 \Phi_L^2(y') \xi(\text{Re}_L(y'), \bar{\Delta}) \frac{G_L(y')^2}{2DS_{tr}^2\rho_L} \frac{U}{q(y')} dy' + \\ & + \Phi_L^2(1) \frac{\xi(\text{Re}_L, \bar{\Delta})(G_L(1))^2 L_z}{D 2S_{tr}^2\rho_L} + \Delta p U, \quad (3) \\ & \Delta p U = \rho_L (V_L(1))^2 \varphi_L(1) + \\ & + \rho_G (V_G(1))^2 \varphi_G(1) - \rho_L (V_L(0))^2, \end{aligned}$$

where $\varphi_G(1)$ is the true volumetric gas content at the evaporator output [Nigmatulin, 1987a,b], u.f.; $\varphi_L(1)$ is the true volumetric liquid content at the evaporator output, u.f.; $\Phi_L^2(1)$ is the dimensionless empirical correction coefficient; $\xi(\text{Re}_L, \bar{\Delta})$ is the friction drag depending on Reynolds number and relative roughness of the tube surface; D is the tube diameter, m; S_{tr}^2 is the tube cross section area, m²; $G_L(y)$ is the flow rate of liquid within the tube length y , L/h; q is the heat flux per tube unit length, W/m; L_y is the path length

between the accelerator output and the confluence of the G_x and G_y flows (node), m; L_z is the path length from the evaporator output to the accelerator input, m; L_{un} is the path length from the node to the evaporator input, m; $V_L(0)$ and $V_L(1)$ are the true liquid flow velocities at the evaporator input and output, m/s; $V_G(1)$ is the true gas velocity at the evaporator output, m/s; Δp is the pressure gradient due to acceleration of the liquid-gas mixture, Pa; ρ_G is the density of gaseous fluid, kg/m³.

The first term in (3) refers to the pressure gradient in the liquid between the accelerator output and the evaporator input; the second term corresponds to the total pressure gradient required to overcome friction within the tube segment filled with liquid only; the third term accounts for the pressure drop to zero due to friction within the phase transition segment; the fourth term is the pressure gradient required to overcome friction in the tubes; and the fifth term is the pressure gradient due to acceleration of the gas-liquid mixture.

The derivation for $\xi(\text{Re}_L, \bar{\Delta})$ and Φ_L^2 was detailed earlier [Idelchik, 1992; Anikin et al., 2011].

Since it is the error in the y_{max} path length that most likely causes misfit between measured and computed average evaporator temperatures, equation (2) has to be corrected for excess fluid temperature:

$$y_{max} = \left(\frac{\rho_L g H_{con} - \Delta p}{dP_{sat}/dt_{con}} + dt_{ex} \right) \frac{C_{pL} G_L}{U}, \quad (4)$$

where dt_{ex} is the excess temperature, °C. The new parameter dt_{ex} is the temperature excess relative to the phase change point, before the boiling starts and, hence, before the gas phase appears in the fluid flow.

The trend with a least-square approximation $y = kx + b$, and dt_{ex} was selected such that the coefficient b in the trend equation reduced to zero, i.e., the theory fully coincided with the experiment (Fig. 4). For this, the excess temperature was specified as a linear series with the values $dt_{ex} = [0.0; 2.5; 5.0; 7.5]$ °C, and the operation of the HET system was modeled for each value, with the input parameters corresponding to the specific experimental run (Table 1). According to the modeling results (Table 3), the average evaporator temperature changes linearly as a function of dt_{ex} . The next step consisted in search of the best-fit dt_{ex} value using the *Tendency* option in *Microsoft Office Excel*. Thus dt_{ex} values were found for each run (Table 4).

To properly check the quality of the experimental results, the HET system has to reach certain operation stability, which was not the case in all runs (Table 4). For instance, excess temperature in run 1 was only 1.34 °C, possibly because the system had not attained stable operation yet. The high excess tem-

Table 3. Average evaporator temperature as a function of excess temperature (dt_{ex}), at input parameters of specific runs

| No. | L_{ev} , m | H_{con} , m | q , W/m | t_{con} , °C | t_{exp} , °C | dt_{ex} , °C | | | |
|-----|--------------|---------------|-----------|----------------|----------------|------------------------------------|--------|--------|--------|
| | | | | | | 0.0 | 2.5 | 5.0 | 7,5 |
| | | | | | | Average evaporator temperature, °C | | | |
| 1 | 800 | 3.00 | 9.46 | -2.25 | -0.87 | -1.54 | -0.29 | 0.96 | 2.21 |
| 2 | 400 | 0.86 | 11.85 | -1.99 | -0.53 | -1.78 | -0.53 | 0.72 | 1.97 |
| 3 | 200 | 1.80 | 28.55 | -6.50 | -4.67 | -5.98 | -4.73 | -3.48 | -2.24 |
| 4 | 400 | 0.86 | 9.50 | -3.70 | -2.06 | -3.47 | -2.22 | -0.97 | 0.28 |
| 5 | 400 | 0.86 | 13.47 | 11.75 | 13.42 | 11.89 | 13.14 | 14.39 | 15.64 |
| 6 | 400 | 1.67 | 14.03 | 8.61 | 10.50 | 8.91 | 10.16 | 11.41 | 12.66 |
| 7 | 600 | 3.00 | 12.05 | -4.25 | -1.82 | -3.48 | -2.23 | -0.98 | 0.27 |
| 8 | 600 | 1.80 | 9.35 | -3.75 | -1.54 | -3.29 | -2.04 | -0.79 | 0.46 |
| 9 | 200 | 3.00 | 32.50 | -5.00 | -2.18 | -4.16 | -2.91 | -1.67 | -0.42 |
| 10 | 400 | 3.00 | 31.68 | -10.50 | -5.95 | -9.67 | -8.40 | -7.14 | -5.88 |
| 11 | 200 | 3.00 | 57.10 | -15.00 | -9.05 | -13.92 | -12.67 | -11.42 | -10.17 |
| 12 | 400 | 1.67 | 21.89 | 11.98 | 17.37 | 12.24 | 13.49 | 14.74 | 15.99 |
| 13 | 200 | 1.80 | 48.10 | -15.00 | -8.65 | -14.35 | -13.10 | -11.85 | -10.60 |

Table 4. Fluid excess temperatures for each run

| No. | L_{ev} , m | H_{con} , m | q , W/m | t_{con} , °C | t_{exp} , °C | Fluid excess temperature, °C |
|-----|--------------|---------------|-----------|----------------|----------------|------------------------------|
| 1 | 800 | 3.00 | 9.46 | -2.25 | -0.87 | 1.34 |
| 2 | 400 | 0.86 | 11.85 | -1.99 | -0.53 | 2.50 |
| 3 | 200 | 1.80 | 28.55 | -6.50 | -4.67 | 2.63 |
| 4 | 400 | 0.86 | 9.50 | -3.70 | -2.06 | 2.82 |
| 5 | 400 | 0.86 | 13.47 | 11.75 | 13.42 | 3.07 |
| 6 | 400 | 1.67 | 14.03 | 8.61 | 10.50 | 3.18 |
| 7 | 600 | 3.00 | 12.05 | -4.25 | -1.82 | 3.32 |
| 8 | 600 | 1.80 | 9.35 | -3.75 | -1.54 | 3.50 |
| 9 | 200 | 3.00 | 32.50 | -5.00 | -2.18 | 3.98 |
| 10 | 400 | 3.00 | 31.68 | -10.50 | -5.95 | 7.36 |
| 11 | 200 | 3.00 | 57.10 | -15.00 | -9.05 | 9.74 |
| 12 | 400 | 1.67 | 21.89 | 11.98 | 17.37 | 10.27 |
| 13 | 200 | 1.80 | 48.10 | -15.00 | -8.65 | 11.41 |

 Table 5. Results of physical-mathematical modeling for HET system operation, with $dt_{ex} = 3.125$ °C

| No. | L_{ev} , m | H_{con} , m | q , W/m | t_{con} , °C | t_{exp} , °C | t_{theor} , °C |
|-----|--------------|---------------|-----------|----------------|----------------|------------------|
| 1 | 400 | 0.86 | 11.85 | -1.99 | -0.53 | -0.22 |
| 2 | 200 | 1.80 | 28.55 | -6.50 | -4.67 | -4.42 |
| 3 | 400 | 0.86 | 9.50 | -3.70 | -2.06 | -1.91 |
| 4 | 400 | 0.86 | 13.47 | 11.75 | 13.42 | 13.45 |
| 5 | 400 | 1.67 | 14.03 | 8.61 | 10.50 | 10.47 |
| 6 | 600 | 3.00 | 12.05 | -4.25 | -1.82 | -1.91 |
| 7 | 600 | 1.80 | 9.35 | -3.75 | -1.54 | -1.73 |
| 8 | 200 | 3.00 | 32.50 | -5.00 | -2.18 | -2.60 |

peratures in runs 10–13 (7.36–11.41 °C) may indicate too high thermal loads on the evaporator, with high probability that the fluid would consist of a single gas phase at the evaporation output during stable operation, i.e., the system will reach the upper critical thermal load for the given HET configuration [Melnikov et al., 2017]. Therefore, those runs should be excluded from the consideration.

Then, taking into account possible errors, the average excess temperature (overheating) of the working fluid in all remaining runs can be estimated as $dt_{ex} = 3.125$ °C. This value is assumed to be the true excess fluid temperature for all configurations of the HET system charged with ammonia. The solutions to the physical-mathematical model corrected for this temperature excess are listed in Table 5.

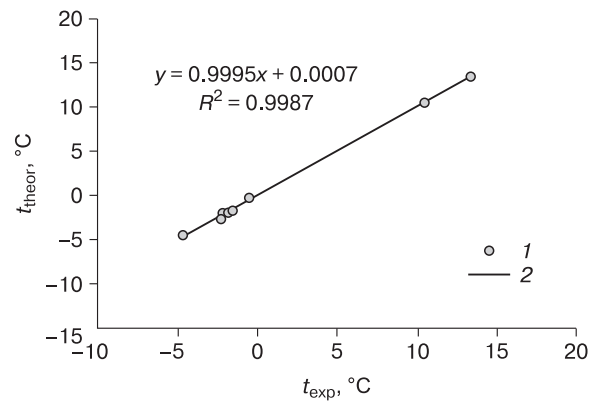


Fig. 5. Measured (t_{exp}) and computed (t_{theor}) average evaporator temperatures (1) and their least square approximation (2), corrected for excess temperature.

In Fig. 5, thus estimated and corrected average evaporator temperatures are compared with the measured values. The coefficient b has been obviously reduced to zero (Fig. 5), i.e., the correction has led to a perfect fit between the computed and measured values; the trend slope is 44.99° .

The results of this study provide more rigorous constraints on temperature variations during the operation of HET systems. The obtained evaporator temperatures are slightly higher than in the previous studies [Anikin, 2009; Anikin et al., 2011; Melnikov et al., 2017] because the fluid overheats before the boiling point.

The revealed relationship between the parameters unambiguously determines the behavior of the system, at both high and low condenser temperatures.

CONCLUSIONS

1. A new parameter of fluid overheating (excess temperature) has been introduced into the existing physical-mathematical model to describe the operation of HET systems. The respective correction led to a 1.57°C higher average evaporator temperature calculated with the model.

2. The excess temperature of the working fluid (ammonia) is 3.125°C , which is reliable for HET systems of various configurations, with the 0.86 to 3.0 m condenser heights; 200 to 600 m tube lengths; -6.50 to 11.75°C condenser temperatures; and 9.35 to 32.50 W/m specific thermal loads.

3. The approximation of the obtained relationship between computed and measured average evaporator temperatures is reliable to 99.87 %, at a trend coefficient of $k = 0.9995$, i.e., almost zero error. Therefore, the physical-mathematical model provides an unambiguous description for the system operation at both positive and negative condenser temperatures.

References

- Anikin, G.V., 2009. Simulating the Operation of Cooling Systems with Horizontal Evaporator Tubes. IKZ, Moscow, Deposited at VINITI 30.10.2009, No. 674-V2009. (in Russian)
- Anikin, G.V., Plotnikov, S.N., Spasennikova, K.A., 2011. Computer simulation of heat-mass exchange in the systems of horizontal ground cooling. *Kriosfera Zemli* XV (1), 33–39.
- Dolgikh, G.M., Okunev, S.N., 1989. Nature Conservation Measures, Environment-Friendly Technologies, and Equipment for Development of New Gas and Condensate Fields in the Yamal Peninsula. Research Activity Report. Giprotyumenneftegaz, Tyumen, 152 pp. (in Russian)
- Dolgikh, G.M., Okunev, S.N., Podenko, L.S., Feklistov, V.N., 2008. Stability, high performance, and manageability of systems for thermal stabilization of permafrost under buildings and engineering structures, in: Resources of Polar and Highland Areas. State and Prospects of Geocryology. Proc. Intern. Conf. Book 2, Tyumen', pp. 34–39.
- Feklistov, V.N., Dolgikh, G.M., Okunev, S.N., Pazderin, D.S., 2008. Investigation into HET thermosyphons for soil stabilization, in: Resources of Polar and Highland Areas. State and Prospects of Geocryology. Proc. Intern. Conf. Book 2, Tyumen', pp. 165–168.
- Idelchik, I.E. (Ed.), 1992. Hydraulic Resistance. A Handbook. Mashinostroenie, Moscow, 616 pp. (in Russian)
- Kutepov, A.M., Sterman, A.S., Stiushin, A.G., 1986. Fluid Dynamics and Heat Transfer in Vapor Formation. Vysshaya Shkola, Moscow, 448 pp. (in Russian)
- Melnikov, V.P., Anikin, G.V., Ishkov, A.A., Plotnikov, S.N., Spasennikova, K.A., 2017. Maximum and minimum critical thermal loads constraining the operation of thermosyphons with horizontal evaporator tubes (HET). *Earth's Cryosphere (Kriosfera Zemli)* XXI (3), 38–44.
- Nigmatulin, R.I., 1987a. Dynamics of Multi-Phase Media. Book I. Nauka, Moscow, 464 pp. (in Russian)
- Nigmatulin, R.I., 1987b. Dynamics of Multi-Phase Media. Book II. Nauka, Moscow, 360 pp. (in Russian)
- Pioro, I.L., Antonenko, V.A., Pioro, L.S., 1991. Efficient Heat Exchange Systems with Two-Phase Thermosyphons. Naukova Dumka, Kiev, 246 pp. (in Russian)

Received October 24, 2017